Usefulness of Cone-Beam Computed Tomography During Ultraselective Transcatheter Arterial Chemoembolization for Small Hepatocellular Carcinomas that Cannot be Demonstrated on Angiography.

Miyayama S, **Yamashiro M**, **Okuda M**, **Yoshie Y**, **Sugimori N**, **Igarashi S**, **Nakashima Y**, **Matsui O**.

Department of Diagnostic Radiology, Fukuiken Saiseikai Hospital, 7-1 Funabashi, Wadanaka-cho, Fukui, 918-8503, Japan, s-miyayama@fukui.saiseikai.or.jp.

This study evaluated the usefulness of cone-beam computed tomography (CBCT) during ultraselective transcatheter arterial chemoembolization (TACE) for hepatocellular carcinomas (HCC) that could not be demonstrated on angiography. Twenty-eight patients with 33 angiographically occult tumors (mean diameter 1.3 +/- 0.3 cm) were enrolled in the study. The ability of CBCT during arterial portography (CBCTAP), during hepatic arteriography (CBCTHA), and after iodized oil injection (LipCBCT) to detect HCC lesions was retrospectively analyzed. The technical success of TACE was divided into three grades: complete (the embolized area included the entire tumor with at least a 5-mm wide margin), adequate (the embolized area included the entire tumor but without a 5-mm wide margin in parts), and incomplete (the embolized area did not include the entire tumor) according to computed axial tomographic (CAT) images obtained 1 week after TACE. Local tumor progression was also evaluated. CBCTAP, CBCTHA, and LipCBCT detected HCC lesions in 93.9% (31 of 33), 96.7% (29 of 30), and 100% (29 of 29) of patients, respectively. A single branch was embolized in 28 tumors, and 2 branches were embolized in five tumors. Twenty-seven tumors (81.8%) were classed as complete, and 6 (18.2%) were classed as adequate. None of the tumors were classed as incomplete. Twenty-five tumors (75.8%) had not recurred during 12.0 +/- 6.2 months. Eight tumors (24.2%), 5 (18.5%) of 27 complete success and 3 (50%) of 6 adequate success, recurred during 10.1 +/- 6.2 months. CBCT during TACE is useful in detecting and treating small HCC lesions that cannot not be demonstrated on angiography.

PMID: 19067043 [PubMed - as supplied by publisher]

Hepatol Res. 2008 Nov 25. [Epub ahead of print]

Histopathological findings after ultraselective transcatheter arterial chemoembolization for hepatocellular carcinoma.

Miyayama S, **Mitsui T**, **Zen Y**, **Sudo Y**, **Yamashiro M**, **Okuda M**, **Yoshie Y**, **Sanada T**, **Notsumata K**, **Tanaka N**, **Matsui O**.

Department of Diagnostic Radiology, Fukuiken Saiseikai Hospital, Fukui, Japan.

Aim: To evaluate the histopathologic findings in the surgical specimen of hepatocelluar carcinoma after transcatheter arterial chemoembolization (TACE) at the most distal portion of the sub-subsegmental artery of the liver (ultraselective TACE). Methods: Histolopathologic findings from nine tumors with a mean diameter of 3.1 cm +/- 1.7 from patients who underwent hepatectomy after ultraselective TACE were evaluated, especially with regard to the relationship between peritumoral liver parenchymal necrosis and portal vein visualization during TACE. Portal vein visualization was classified into three grades by a spot digital radiograph obtained just after TACE: 0, no obvious portal vein visualization; 1, visualization of the portal vein adjacent to the tumor; and 2, visualization in the whole embolized area or extending into the surrounding non-embolized areas. Unenhanced computed tomography (CT) was obtained 1 week later and surgical resection was performed 37 +/- 6.3 days after ultraselective TACE. Results: Portal vein visualization during TACE was classed as grade 1 in 5 tumors and grade 2 in 4. Histopathologically, complete tumor necrosis was observed in 7 tumors (77.8%). In 2 tumors (1 of grade 1, the other grade 2), a small viable portion or viable daughter nodule was seen. Macroscopic parenchymal necrosis adjacent to the tumor was observed in all 4 grade 2 tumors including gas-containing areas on CT obtained 1 week after TACE. Conclusions: Ultraselective TACE induces not only complete tumor necrosis but also peritumoral parenchymal necrosis, similar to that after radiofrequency ablation, when the portal veins are markedly visualized during the TACE procedure.

PMID: 19054146 [PubMed - as supplied by publisher]

Eur Radiol (2008) 18: 1918–1924
DOI 10.1007/s00330-008-0954-5

Rieko Shinmura
Osamu Matsui
Masumi Kadoya
Satoshi Kobayashi
Noboru Terayama
Junichiro Sanada
Hiroshi Demachi
Toshifumi Gabata

Detection of hypervascular malignant foci in borderline lesions of hepatocellular carcinoma: comparison of dynamic multi-detector row CT, dynamic MR imaging and superparamagnetic iron oxide-enhanced MR imaging

Received: 25 October 2007
Revised: 22 January 2008
Accepted: 25 February 2008
Published online: 2 April 2008

R. Shinmura (✉) · H. Demachi
Department of Radiology,
Toyama Prefectural Central Hospital,
2-2-78 Nishinagae,
Toyama, 930-8550 Japan
e-mail: rieko@rad.m.kanazawa-u.ac.jp
Fax: +81-76-4220667

O. Matsui · S. Kobayashi ·
N. Terayama · J. Sanada · T. Gabata
Department of Radiology, Kanazawa
University School of Medicine,
Kanazawa, 920-8641 Japan

M. Kadoya
Department of Radiology, Shinshu
University School of Medicine,
Matsumoto, 390-8621, Japan

Abstract The study object was to retrospectively compare the detection rate of hypervascular foci visualized by CT during hepatic arteriography (CTHA) in borderline nodules, which was observed upon cirrhotic livers, on dynamic MDCT, dynamic gadolinium-enhanced MR (dynamic MR), and SPIO-enhanced MR imaging. Eighty-five nodules in 49 patients with cirrhosis were evaluated. When a part of the nodule showed hyperdensity relative to the surrounding areas of the nodule on CTHA, it was defined as "hypervascular focus." The relationships between the dynamic MDCT and dynamic MR and SPIO-enhanced MR imaging findings of these foci were analyzed using X^2 test. Hypervascular foci were detected in 17 (53%) of 32 on the arterial dominant phase of dynamic MDCT, in 19 (37%) of 51 on the arterial dominant phase of dynamic MR and in 6 (26%) of 23 on SPIO-enhanced MR imaging. Arterial dominant phase of dynamic MDCT demonstrated a significantly higher detection rate of hypervascular foci less than 5 mm in diameter than did dynamic and SPIO MR imaging ($p<0.05$). Hypervascular foci in borderline nodules could be better visualized by dynamic MDCT than by gadolinium- and SPIO-enhanced MR imaging. Dynamic MDCT is recommended for the follow-up examination of hypovascular borderline lesions.

Keywords Liver · Malignant foci · Hepatocellular carcinoma · Computed tomography · MR imaging

Introduction

Patients with chronic hepatitis or cirrhosis, especially hepatitis C- or B-related liver cirrhosis, are at increased risk of developing hepatocellular carcinoma (HCC), and early detection of HCC is mandatory for their optimal management. In patients with cirrhosis, various kinds of hepatocellular nodules, ranging from regenerative nodules to HCC, are often found. As previously reported, these hepatocellular nodules are divided into several histologic groups, namely adenomatous hyperplasia (AH), atypical AH, early HCC, well-differentiated HCC and moderately or poorly differentiated HCC [1–5] according to the classification of the Japan Liver Cancer Study Group [6]. AH is considered to correspond to low-grade dysplastic nodule (DN) and atypical AH and a part of early HCC with high-grade DN in the classification of the World Congress of Gastroenterology [7]. In these nodules, multi-step human hepatocarcinogenesis from high-grade DN to HCC has been well documented [8, 9]. However, because the histological features of these nodules are sequential, and internal histological heterogeneity is often seen in them, the precise differential diagnosis between borderline lesions and early stage highly well-differentiated HCC (early HCC) is often difficult even by histological examination. As a result, the imaging findings of these two are similar and overlap, typically showing hypovascularity on dynamic CT, dynamic MR imaging, and contrast ultrasound and internal portal blood supply on CT during arterial portography (CTAP). However, this kind of hypovascular early stage well-differentiated HCC does not demonstrate definite metastasis or vascular invasion and is biologically benign. Therefore, in clinical practice, predicting the transformation of these hypovascular

nodules to hypervascular HCC by non-invasive imaging procedures is important.

We previously verified the stepwise changes of the intranodular blood supply in parallel with the elevation of the grade of malignancy of these hepatocellular nodules [2, 10]. We also revealed an intense correlation between the patterns of intranodular blood supply and prognosis of the nodules [11]. According to our analysis by CTAP and CT during hepatic arteriography (CTHA), all of the entirely hypovascular nodules showing internal hypervascular foci demonstrated progression to entirely hypervascular classical HCC [11]. Therefore, to detect a hypervascular focus in a hypovascular borderline lesion is very important clinically, because it indicates definite malignant transformation from biologically benign hepatocellular nodule (borderline lesion or early HCC) to invasive classical HCC.

The purpose of this study was to assess the efficacy of dynamic CT using a multidetector CT system, dynamic MR imaging, and superparamagnetic iron-oxide (SPIO)-enhanced MRI in the detection of hypervascular foci in hypovascular borderline lesions of HCC visualized by CT during hepatic arteriography (CTHA).

Materials and methods

Successive 85 nodules in 49 patients showing a hypervascular focus in a borderline lesion diagnosed by CTHA and CT during arterial portography (CTAP) during the period from April 1999 to May 2006 were the focus in the study. The study comprised 36 men and 13 women ranging in age from 42 to 83 years (mean age, 67 years). All patients had associated liver cirrhosis, which was hepatitis B virus-related cirrhosis in five patients, hepatitis C virus-related in 40, both hepatitis B- and C-related in 2, alcoholic in 1 and autoimmune in 1. The size of the borderline lesions ranged from 10 to 30 mm in diameter (average 17 mm), and those of the hypervascular foci were 2 to 15 mm (average 6 mm). All measurements were performed on CTHA images, and the largest diameter was employed for the analysis. Hypervascular foci less than 5 mm were diagnosed by the combination of imaging findings including CTAP and CTHA and more than 6 months' follow-up showing enlargement of the foci.

Regarding these nodules, the detectability of a hypervascular focus by dynamic CT, dynamic MRI, and SPIO-enhanced MR imaging performed within 2 weeks before or after CTAP, and CTHA examinations was analyzed. Informed consent for each examination and retrospective analysis of the imaging findings was obtained from all patients. No institutional approval was needed for this kind of retrospective analysis of imaging findings at our institution.

Dynamic CT was carried out in 32 nodules in 17 patients, dynamic MRI in 51 nodules in 31 patients, and SPIO-enhanced MRI in 23 nodules in 17 patients. Each image was analyzed retrospectively in comparison with the CTAP and CTHA findings. CT was performed in all cases, however, because we introduced multi-detector-row CT in April 2002, only 17 patients were subjected to the study. MRI and SPIO-enhanced MRIs were carried out in the selected cases case by case based on the ragiologists decision for further detection and characterization of HCCs.

CTAP and CTHA examinations

CTAP and CTHA were performed after hepatic angiography using a combined digital subtraction angiography (DFP 2000 A; Toshiba, Japan) and helical CT (Xvision SP; Toshiba) system. After femoral artery puncture, a 4-French catheter was selectively placed in the superior mesenteric artery for CTAP and in the common or proper hepatic artery for CTHA. For CTAP, 5-mm collimation and a 7-mm/s table speed were used. The duration of CT data acquisition was approximately 20 s during a single breath hold for a total cranio-caudal coverage of 14–18 cm. Overlapping reconstructions were obtained every 2.5 mm. Helical CT began 25 s after the beginning of an infusion of 60 ml of iohexol (320 mg of iodine per milliliter) (Omnipaque; Daiichi, Tokyo, Japan) at 2 ml/s, and 5 μg of prostaglandin E1 (Palux; Taisyo, Tokyo, Japan) was injected into the superior mesenteric artery immediately before the injection of contrast medium. Approximately 10 min after CTAP was performed, CTHA was obtained with 5-mm collimation, a 6-mm/s table speed, and 2.5-mm reconstruction intervals. CTHA began 10 s after the start of the injection of iohexol (320 mg of iodine per milliliter) at 2 ml/s. The infusion was continued throughout the CT data acquisition. In all patients, conventional CT (including non-enhanced CT) was performed separately, on a different day, before the CTAP and CTHA procedures. The angiographic procedures were performed by radiologists who each had more than 8 years of experience performing abdominal angiography (R.S., O.M., S.K., N.T., J.S., K.U.).

Multi–detector-row CT

CT examinations were performed using a 16–detector-row CT system (LightSpeed Ultra; GE Medical Systems). Images were acquired through the liver in a craniocaudal direction with a 1.5×16 beam collimation. Other CT parameters were as follows: 150 mAs; 120 kVp; detector collimation, 2.5 mm; table speed, 14 mm per rotation; gantry rotation time, 0.5 s. A reconstruction section thickness of 2.5 mm and a reconstruction interval of 2.5 mm were used. Before the examinations, patients were instructed to hold their breath to avoid motion artifacts. Unenhanced multi–detector row CT was performed first. For dynamic CT, contrast medium with a concentration of

320 mg of iodine per milliliter (Omnipaque, Daiichi, Tokyo, Japan) was administered with a power injector. The total volume of 100 ml was injected at a rate of 3 ml/s through a 21-gauge plastic intravenous catheter that was placed in an antecubital vein. Thirty-five seconds after initiation of the injection, the early arterial phase CT acquisition began. The dynamic images consisted of three phases (i.e., arterial dominant, portal dominant and equilibrium phases).

MR imaging

MR imaging was performed with a 1.5-T MR imaging unit (Signa Horizen; GE Medical Systems, Milwaukee, WI). All images were obtained in the transverse plane by using a phased-array multicoil. The matrix size was 128×256 or 256×256. The following unenhanced MR imaging examinations were performed: Respiratory-triggered fast spin-echo T2-weighted imaging [4,000/90 ms (repetition time ms/echo time ms), two acquisitions] was performed with frequency selective fat saturation, a section thickness of 8 mm, and a 2-mm intersection gap. Respiratory compensation spin-echo T1-weighted imaging (500/9, two acquisitions) was performed using a section thickness of 8 mm and a 2-mm intersection gap. Breath-hold T1-weighted fast multiplanar spoiled gradient-recalled-echo in-phase (150–200/4.4, one acquisition) and out-of-phase (120–180/2.2, one acquisition) imaging examinations were performed with a flip angle of 90°, an 8-mm section thickness, and a 2-mm intersection gap. The hepatocellular nodule signal intensities evaluated at the respiratory-triggered fast spin-echo T2-weighted and respiratory compensation spin-echo T1-weighted examinations were used in our analysis.

For gadolinium-enhanced dynamic imaging, gadopentetate dimeglumine (Magnevist; Schering, Berlin, Germany) was injected as a rapid bolus by hand injection at a dose of 0.1 mmol/kg and immediately followed by a 10–20 ml saline flush. The dynamic T1-weighted fast multiplanar spoiled gradient-recalled-echo (150/1.6, one acquisition, fat saturation) imaging examinations were performed with a flip angle of 90°, obtained in the transverse plane during suspended respiration immediately after intravenous injection of the gadolinium chelate, and additional images were obtained at 30–35 s, 65–70 s, and 3 min.

Ferumoxides (Feridex I.V.; Advanced Magnetics, Cambridge, MA) were administered at 15 μmol of iron per kilogram of body weight. The ferumoxide suspension was diluted in 100 ml of a 5% glucose solution and administered intravenously for 30 min. Patients underwent enhanced MR imaging 30 min after the administration of the contrast agent. SPIO-enhanced MR imaging was performed with the following sequences: respiratory-triggered T2-weighted FSE sequence and breath-hold T2*-weighted GRE sequence with 150/13, a 60° and 20° flip angle. The respiratory-triggered T2-weighted FSE MR images were obtained using the same parameters used to obtain the unenhanced images. To confirm the diagnosis of arterioportal shunt and characterization of HCC, we performed MR imaging using ferumoxides.

Image evaluation

The diagnosis of a "borderline lesion" was made when intranodular portal supply was demonstrated on CTAP, and decreased arterial supply relative to the surrounding liver was shown on CTHA in more than half of the nodule. When a part of the nodule showed hyperdensity relative to the surrounding areas of the nodule on CTHA, it was defined as a "hypervascular focus."

All images were interpreted retrospectively by three experienced radiologists (R.S., O.M., S.K., one with more than 8 and the other two with more than 17 years of experience in liver imaging). CT and MR imaging findings were evaluated without knowing the findings of the other imaging examination, and images were analyzed subjectively and independently by these three radiologists. Disagreements were resolved by consensus. Interobserver correlation was not analyzed because of the simplicity of image interpretation.

Statistical analysis

Statistical analysis was performed using χ^2 test for evaluating the association between the modalities and a malignant focus, and the observed significant level was calculated by the two-tailed test. Moreover, statistical analysis of each combination was performed using the Bonferoni test. Differences were considered significant when the P value was less than 0.05. All statistical analyses were performed using a statistical software package (SPSS 11.0J for Windows; SPSS, Chicago, IL).

Results

CT demonstrated all 32 nodules examined, with a hypervascular focus less than 5 mm in the largest diameter on CTHA seen in 19 nodules and more than 5 mm in the remaining 13 nodules. On unenhanced CT, the hypervascular focus was not identified in any of the nodules. On the arterial dominant phase of dynamic CT, the hypervascular focus was detected in 17 of total 32 nodules (53%) (Fig. 1) (Table 1). A hypervascular focus less than 5 mm was visualized in 6 of 19 nodules (32%) and more than 5 mm in 11 of 13 nodules (83%). On the portal and equilibrium phases of dynamic CT, a malignant focus was not identified in any nodules.

MR imaging demonstrated all 51 nodules examined, in which a hypervascular focus less than 5 mm in the largest

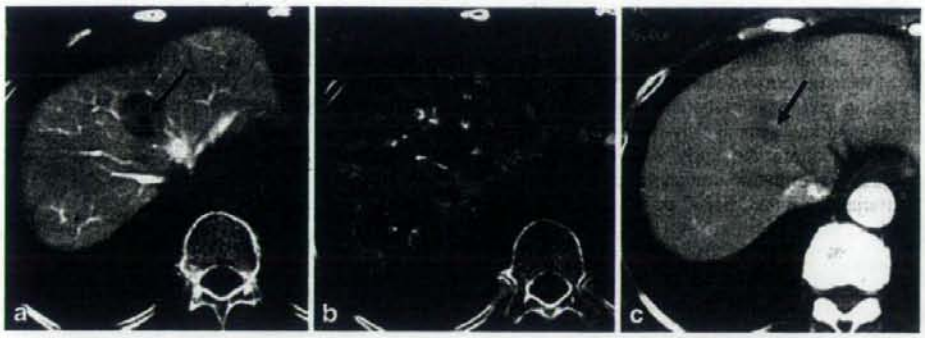

Fig. 1 A 75-year-old man with liver cirrhosis **a**. Transverse CTAP shows a spotty hypoattenuating area within a slightly hypoattenuating nodule in liver segment IV/VIII. **b** Transverse CTHA shows a spotty hyperattenuating area within the isoattenuating nodule. **c** Transverse on the arterial dominant phase of dynamic CT shows a hypervascular focus within a slightly hypoattenuating nodule

diameter on CTHA was seen in 29 nodules and more than 5 mm in the remaining 22 nodules. On T1-weighted images, the entire nodule was hyperintense in 33 nodules (65%), isointense in 13 (25%), and hypointense in 3 (6%). The hypervascular focus was visualized as a spotty hyperintense area within an isointense nodule in the remaining two nodules (4%) (Fig. 2). On T2-weighted images, the entire nodule was hyperintense in 10 nodules (20%), isointense in 24 (47%), and hypointense in 11 (22%). The hypervascular focus was detected in the remaining six nodules (12%) showing a spotty hyperintense area within the hypointense or isointense nodule (Fig. 3). On the arterial dominant phase of gadolinium-enhanced dynamic MR imaging, the hypervascular focus was identified as a hyperintense area within the nodule in 19 of 51 nodules (37%) (Fig. 4). A hypervascular focus less than 5 mm was detected in 5 of 29 nodules (17%) and more than 5 mm in 14 of 22 nodules (64%) (Table 1).

On SPIO-enhanced MR imaging, the hypervascular focus was demonstrated in 6 of 23 nodules examined (26%) as a hyperintense area in a hypointense or isointense nodule (Fig. 5). The hypervascular focus less than 5 mm in the largest diameter on CTHA was detected in 1 of 12 nodules (8%) and more than 5 mm in 5 of 11 nodules (45%). In the remaining 17 nodules, the entire nodule was hyperintense in 6 nodules (26%), isointense in 7 (30%), and hypointense in 4 (17%).

The mean largest diameter of the hypervascular foci detected on the arterial dominant phase of dynamic CT was 6.4 mm, and the ratio of its area to the entire nodule was 38%. They were 8.2 mm and 39% on the arterial dominant phase of dynamic MRI and 8.3 mm and 36% on SPIO-enhanced MRI, respectively. There was no significant difference in the diameter or ratio of its area to the entire nodule among these modalities.

Arterial dominant phase of dynamic CT detected a significantly higher proportion of the hypervascular foci less than 5 mm in diameter than did dynamic MRI and SPIO-enhanced MRI ($P<0.05$). However, in the detection rates of hypervascular foci more than 5 mm in diameter, there were no significant differences between these various techniques (Table 1). There was no significant difference in the detection ratio of the hypervascular foci between the arterial dominant phase of dynamic MRI and SPIO.

Table 1 Detectability of hypervascular focus

	Dynamic CT arterial phase (n=32)	Dynamic MRI arterial phase (n=51)	SPIO-enhanced MRI (n=23)
Size ≥5 mm	6/19 (32)	5/29 (17)	1/12 (8)
<5 mm	11/13 (83)	14/22 (64)	5/11 (45)

Discussion

In Japan, more than 90% of HCCs are associated with hepatitis B or C virus infection, notably 70% with hepatitis C. Therefore, it has become possible to detect small early stage HCCs by periodic imaging of patients with these high-risk diseases. However, various kinds of borderline hepatocellular nodules as described above are also often detected at the same time [15, 16]. It is well known that cancerous foci of HCC are occasionally encountered within high-grade DN, called a DN with subfocus of HCC. In

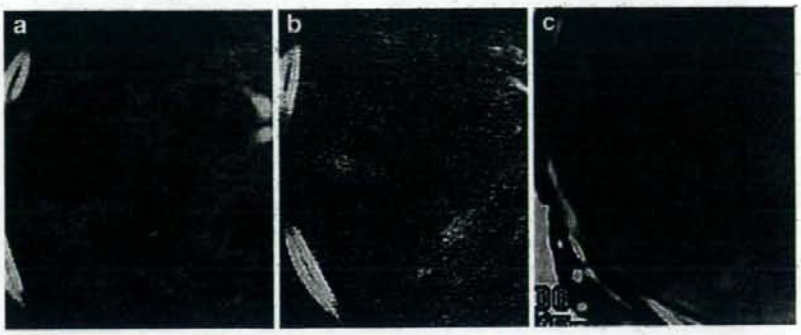

Fig. 2 A 68-year-old man with liver cirrhosis **a**. Transverse CTAP shows a hypoattenuating nodule in liver segment V. **b** Transverse CTHA shows a spotty hyperattenuating area within a hypoattenuating nodule. **c** Transverse T1-weighted MR image shows a hyperintense focus within an isointense nodule

these nodules, two types of human hepatocarcinogenesis are now considered to occur. One is de novo hepatocarcinogenesis and the other is the stepwise development from high-grade DN, high-grade DN with well-differentiated HCC foci, and overt HCC.

We previously described that the intranodular blood supply evaluated by CTAP and CTHA changed in accordance with hepatocarcinogenesis, from DN to overt HCC [9, 10]. In parallel with increasing elevation of the grade of malignancy of the nodules, the portal tract including the normal portal vein (intranodular portal supply) and hepatic artery (intranodular arterial supply through normal hepatic arteries) is decreased. On the other hand, abnormal artery (intranodular arterial supply through newly formed abnormal arteries) gradually increases [5, 16]. Therefore, we can estimate the grade of malignancy of the nodules from the intranodular blood supply. In DNs, hypovascularity (less arterial vascularity) relative to the surrounding liver is usually seen. On the other hand, typical classical HCCs always show increased arterial supply with absent intranodular portal supply. However, early stage highly well-differentiated HCC demonstrates variable findings, namely hypovascular, isovascular, partially hypervascular and entirely hypervascular (usually faint) [10]. According to our analysis, all of the nodules showing hypervascular foci in entirely hypovascular nodules demonstrated progression to entirely hypervascular nodules (hypervascular classical HCC) within around 900 days (malignant transformation). On the other hand, only around 30% of the nodules without a hypervascular focus progressed to classical HCC during the same period, and all of them revealed the appearance of hypervascular foci in the nodule before the progression to classical HCC [11]. Therefore, to detect a hypervascular focus is important clinically. However, as far as we reviewed, no report has focused on the detectability of a minute hypervascular focus in a hypovascular borderline lesion by non-invasive conventional imaging modalities.

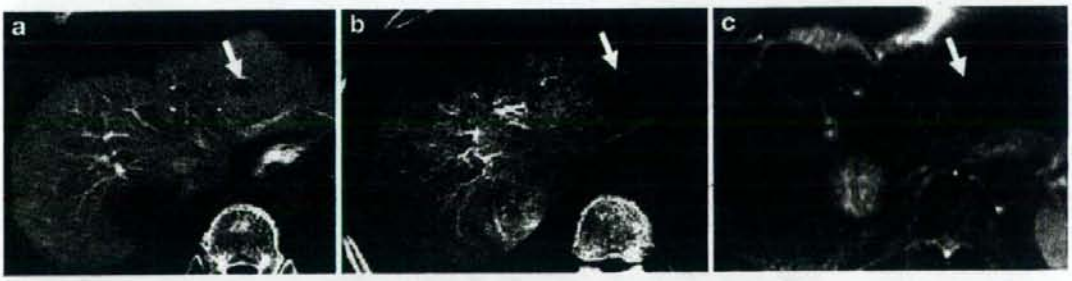

Fig. 3 A 71-year-old man with chronic hepatitis B **a**. Transverse CTAP shows a nodular hypoattenuating area within an isoattenuating large nodule in liver segment III. **b** Transverse CTHA shows a nodular hyperattenuating area within a hypoattenuating large nodule. **c** Transverse T2-weighted MR image shows a hyperintense focus within a slightly hypointense large nodule

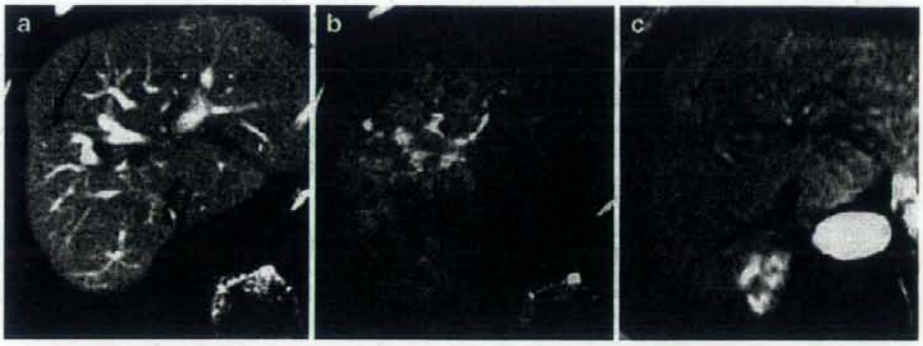

Fig. 4 A 63-year-old woman with liver cirrhosis **a**. Transverse CTAP shows a spotty hypoattenuating area within an isoattenuating nodule in liver segment VIII. **b** Transverse CTHA shows a spotty hyperattenuating area within a hypoattenuating nodule. **c** Transverse on the arterial dominant phase of gadolinium-enhanced dynamic MR image shows a hyperintense focus within an isointense nodule

As shown in this study, CT and MRI without contrast enhancement cannot visualize a hypervascular (malignant) focus in a hypovascular borderline lesion in the majority of cases. Therefore, to visualize it, contrast-enhanced CT or MRI is mandatory. In this study, the detectability of a malignant focus was the best with dynamic CT using MDCT and was relatively poor with SPIO-enhanced MRI. Therefore, at this time, because of the widespread availability of CT, dynamic CT is considered to be the most suitable imaging modality for detecting a hypervascular malignant focus in borderline lesions. However, the ability of these less invasive modalities was not satisfactory, especially for the detection of malignant foci less than 5 mm in diameter.

As far as we could determine, no reports have analyzed the detectability of a hypervascular focus detected by CTHA by various non-invasive imaging techniques, except the one study of Goshima et al. [19]. They compared the detectability of a hypervascular malignant focus by CTHA between gadolinium-enhanced dynamic MR imaging and SPIO-enhanced MR imaging. Their results suggested that nodule-in-nodule appearance of HCC could be seen on SPIO-enhanced MR images, in some cases more clearly than on gadolinium-enhanced MR images, particularly when the background nodule showed hyperintensity on unenhanced T1-weighted images. However, the results for the detection of HCC by MR imaging have a very broad variance, attributable to differences in tumor size, histological grading, differences with regard to cirrhotic livers with impaired function and the fact that some well-differentiated HCC themselves take up SPIO [17, 18]. In the present study, gadolinium-enhanced MRI was superior to SPIO-enhanced MRI in the detection of hypervascular malignant foci larger than 5 mm.

A limitation of our study is the lack of histological proof of all liver lesions, because biopsy is impossible for nodules that are not visible by ultrasound and is often not performed due to the presence of multiple associated lesions. Therefore, the diagnosis was based on long-term follow-up.

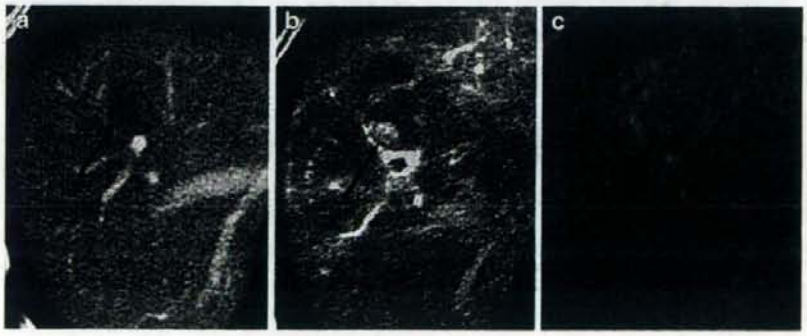

Fig. 5 A 72-year-old woman with liver cirrhosis **a**. Transverse CTAP shows a hypoattenuating area within a slightly hypoattenuating nodule in liver segment VIII. **b** Transverse CTHA shows a hyperattenuating area within a hypoattenuating nodule. **c** Transverse on SPIO-enhanced MR imaging shows a hyperintense focus within an isointense nodule

Conclusion

Hypervascular malignant foci in hypovascular borderline nodules over 5 mm in diameter were better visualized by dynamic CT than by MR imaging or SPIO-enhanced MRI, although the differences between techniques did not reach statistical significance. It was difficult to detect malignant foci less than 5 mm by these non-invasive imaging techniques. Dynamic CT is recommended for the follow-up examination of hypovascular borderline lesions.

References

1. Sakamoto M, Hirohashi S, Shimosato Y (1991) Early stage of multistep hepatocarcinogenesis: adenomatous hyperplasia and early hepatocellular carcinoma. Hum Pathol 22:172–178
2. Matsui O, Kadoya M, Kameyama T et al (1991) Benign and malignant nodules in cirrhotic livers: distinction based on blood supply. Radiology 178:493–497
3. Kudo M, Tomita S, Kashida H et al (1991) Tumor hemodynamics in hepatic nodules associated with liver cirrhosis: relationship between cancer progression and tumor hemodynamic change (in Japanese). Nippon Shokakibyo Gakkai Zasshi 88:1554–1565
4. Sakamoto M, Ino Y, Fujii T et al (1993) Phenotype changes in tumor vessels associated with the progression of hepatocellular carcinoma. Jpn JClin Oncol 23:98–104
5. Ueda K, Terada T, Nakanuma Y, Matsui O (1992) Vascular supply in adenomatous hyperplasia of the liver and hepatocellular carcinoma: a morphometric study. Hum Pathol 23:619–26
6. Liver Cancer Study Group of Japan (1992) The general rules for the clinical and pathological study of primary liver cancer, 3rd edn. Kanahara, Tokyo, pp 32–39
7. International Working Party (1995) Terminology of nodular hepatocellular lesions. Hepatology 22:983–993
8. Sakamoto M, Hirohashi S, Tsuda H et al (1989) Multicentric independent development of hepatocellular carcinoma revealed by analysis of hepatitis B virus integration pattern. Am J Surg Pathol 13:1064–1067
9. Matsui O, Kadoya M, Kameyama T, Yoshikawa J, Arai K, Gabata T, Takashima T, Nakanuma Y, Terada T, Ida M (1989) Adenomatous hyperplastic nodules in the cirrhotic liver: differentiation from hepatocellular carcinoma with MR imaging. Radiology 173:123–6
10. Hayashi M, Matsui O, Ueda K et al (1999) Correlation between the blood supply and grade of malignancy of hepatocellular nodules associated with liver cirrhosis: evaluation by CT during intraarterial injection of contrast medium. AJR 172:969–976
11. Hayashi M, Matsui O, Ueda K et al (2002) Progression to hypervascular hepatocellular carcinoma: Correlation with intranodular blood supply evaluated with CT during intraarterial injection of contrast material. Radiology 225:143–9
12. Nakanuma Y, Terada T, Terasaki S et al (1990) Atypical adenomatous hyperplasia in liver cirrhosis: low-grade hepatocellular carcinoma or borderline lesion? Histopathology 17:27–35
13. Sakamoto M, Hirohashi S, Tsuda H et al (1989) Multicentric independent development of hepatocellular carcinoma revealed by analysis of hepatitis B virus integration pattern. Am J Surg Pathol 13:1064–1067
14. Liver Cancer Study Group of Japan (2000) The general rules for the clinical and pathological study of primary liver cancer, 4th edn. Tokyo, Kanahara, pp 30–34
15. International Working Party (1995) Terminology of nodular hepatocellular lesions. Hepatology 22:983–993
16. Nakanuma Y, Hirata K, Terasaki S, Ueda K, Matsui O (1998) Analytical histopathological diagnosis of small hepatocellular nodules in chronic liver diseases. Histol Histopathol 13:1077–1087
17. Krinsky GA, Lee VS, Theise ND et al (2001) Hepatocellular carcinoma and dysplastic nodules in patients with cirrhosis: prospective diagnosis with MR imaging and explantation correlation. Radiology 219:445–454
18. Amelie ML, Jurgen KW, Kerstin Goepfert RT et al (2005) Hepatocellular carcinoma in cirrhosis: Enhancement patterns at dynamic gadolinium-and superparamagnetic iron oxide-enhanced T1-weighted MR Imaging. Radiology 237:520–528
19. Goshima S, Kanematsu M, Matsuo M et al (2004) Nodule-in-nodule appearance of hepatocellular carcinoma: Comparison of gadolinium-enhanced and fermoxides-enhanced magnetic resonance imaging. J Magn Reson Imaging 20:250–255

Abdom Imaging. 2008 Mar 29. [Epub ahead of print]

Detection of hepatocellular carcinoma by CT during arterial portography using a cone-beam CT technology: comparison with conventional CTAP.

Miyayama S, Matsui O, Yamashiro M, Ryu Y, Takata H, Takeda T, Aburano H, Shigenari N.

Diagnostic Radiology, Fukuiken Saiseikai Hospital, 7-1, Funabashi, Wadanaka-cho, Fukui, Japan, miyayama@fukui.saiseikai.or.jp.

BACKGROUND: To evaluate the detectability of hepatocellular carcinoma (HCC) by computed tomography during arterial portography (CTAP) using cone-beam CT technology (CBCTAP) by comparing it with conventional CTAP. METHODS: Forty-four HCC lesions (mean diameter 1.9 +/- 1.1 cm) of 24 patients who sequentially underwent conventional CTAP and CBCTAP during the same angiography session were evaluated. CBCTAP findings of each tumor were classed into three grades as compared to conventional CTAP: optimal; suboptimal; and nondiagnostic. RESULTS: All CBCTAP images had image artifacts from the catheter placed in the superior mesenteric artery and enhanced portal veins. Additionally, the contrast between HCC lesion and surrounding liver parenchyma of CBCTAP images was less than that of CTAP images. Of the 44 tumors, findings of 31 nodules (mean 2.2 +/- 1.2 cm) (70.5%) were classed as optimal. Eight nodules (mean 1.4 +/- 0.8 cm) (18.2%) were classed as suboptimal. Five nodules (mean 1.0 +/- 0.1 cm) (11.4%) including two located in the outside of field of view were classed as nondiagnostic. CONCLUSION: CBCTAP had sufficient image quality to detect almost all small HCC lesions compared to conventional CTAP and could depict approximately 89% of HCC nodules, including eight suboptimal lesions.

PMID: 18373115 [PubMed - as supplied by publisher]

INTERNAL MEDICINE

□ CASE REPORT □

Hepatocellular Carcinoma with a "nodule-in-nodule" Appearance Reflecting an Unusual Dilated Pseudoglandular Structure

Yusuke Ishida[1], Hiroaki Nagamatsu[2], Hironori Koga[1], Hiroshi Yoshida[2], Masamichi Kojiro[3] and Michio Sata[1]

Abstract

We present a case of hepatocellular carcinoma (HCC), showing an atypical "nodule-in-nodule" appearance on ultrasonogram (US). In general, a "nodule-in-nodule" appearance is found as a hyperechoic tumor containing a hypoechoic nodule. In the present case, however, there was a hyperechoic subnodule in the center of the tumor, which was surrounded by a hypoechoic tumor area. Histologically, the subnodule consisted of moderately differentiated HCC with a markedly dilated pseudoglandular structure, and the outer tumor consisted of well-differentiated HCC with a thin-trabecular pattern. It should be noted that there is a rare HCC with dilated pseudoglandular structure showing the inversed "nodule-in-nodule" appearance.

Key words: liver cancer, nodule-in-nodule, dedifferentiation, pseudogland, ultrasonography

(Inter Med 47: 1215-1218, 2008)
(DOI: 10.2169/internalmedicine.47.0640)

Introduction

Small hepatocellular carcinoma (HCC) is sometimes detected as a hyperechoic nodule by ultrasonography (1, 2). Most of these HCCs consist of well-differentiated cancerous tissues with fatty change (3, 4). During the dedifferentiation process, the well-differentiated HCC tissue with fatty change is often recognized as the outer rim of moderately differentiated HCC tissue, showing a hypo-in-hyper-echoic US finding, which is called the "nodule-in-nodule" appearance (4, 5). Here, we report a case with a hyper-in-hypo-echoic HCC, demonstrating an atypical "nodule-in-nodule" appearance caused by moderately differentiated cancerous tissue with markedly dilated pseudoglandular structure in the center of the tumor.

Case Report

A 51-year-old man was referred to our hospital for a further examination of a liver tumor detected at periodic follow-up of hepatitis C virus antibody-positive chronic hepatitis. Laboratory examination on admission revealed elevated values of PIVKA-II, serum alkaline phosphatase, and gamma glutamyl transpeptidase. Serum levels of α-fetoprotein, aspartate aminotransferase, and alanine aminotransferase, and total bilirubin were normal (Table 1). Ultrasonography (US) demonstrated a hypoechoic tumor, 24×34 mm in size, containing a hyperechoic subnodule (Fig. 1). T2-weighted magnetic resonance (MR) images showed a markedly hyperintense area in the center of the tumor; a finding consistent with the hyperechoic nodule seen on US (Fig. 2). On dynamic MR images, the inner part of the tumor was gradually and weakly enhanced by contrast media, followed by a slow washout. On the other hand, the outer part of the tumor was slightly enhanced only at the delayed phase (Fig. 3). He underwent a right hepatic lobectomy with a biopsy diagnosis of moderately differentiated HCC (Fig. 4). Grossly, the resected tumor, 27×30 mm in size, showed a "nodule-in-nodule" appearance (Fig. 5). Histologically, the inner subnodule consisted of moderately differentiated HCC with a markedly dilated pseudoglandular

[1]Division of Gastroenterology, Department of Medicine, Kurume University School of Medicine, Kurume, [2]Department of Internal Medicine, Yame General Hospital, Yame and [3]Yanagawa Hospital, Yanagawa
Received for publication September 28, 2007; Accepted for publication April 8, 2008
Correspondence to Dr. Yusuke Ishida, ishida_yuusuke@kurume-u.ac.jp

Table 1. Laboratory Findings on Admission

RBC	484×10^4/mm^3	PT	104.5%
Hb	15.5 g/dL	PT-INR	0.97
Ht	45.6%	Hyaluronic acid	84 ng/mL
WBC	2400 /mm^3	$ICGR_{15}$	8.6%
Plt	33.0×10^4/mm^3	BUN	11.7 mg/dL
		Cr	0.56 mg/dL
T.B	0.4 mg/dL	Na	145 mEq/L
AST	36 U/L	K	4.2 mEq/L
ALT	41 U/L	Cl	102 mEq/L
LDH	245 U/L		
ALP	333 U/L	AFP	6.3 ng/mL
γ GTP	198 U/L	PIVKA-II	97 mAU/mL
T.P	8.3 g/dL	CEA	2.9 ng/mL
Alb	4.4 g/dL	CA19-9	51.6 U/mL
T.cho	159 mg/dL	HBs Ag	(-)
		Anti-HCV Ab	(+)

structure. In contrast, the outer tumor consisted of well-differentiated HCC with a thin-trabecular pattern (Figs. 6-8).

Discussion

It is known that a "nodule-in-nodule" appearance in relatively small HCC reflects a dedifferentiation process from well-differentiated to moderately differentiated HCC, and it is frequently depicted on US imaging.

The "nodule-in-nodule" appearance is generally found as a hyperechoic tumor containing a hypoechoic nodule, and it reflects the development of moderately differentiated HCC without fatty change within a well-differentiated HCC showing diffuse fatty change. In the present case, however, moderately differentiated HCC was depicted as a hyperechoic

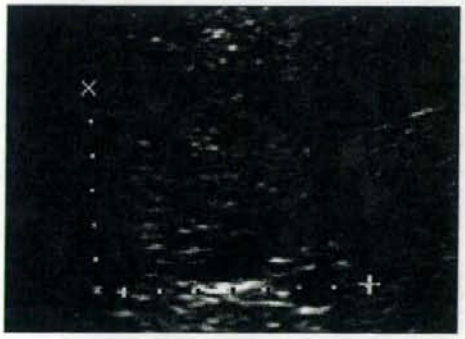

Figure 1. US image of the tumor.

Figure 2. T2-weighted MR images for the tumor.

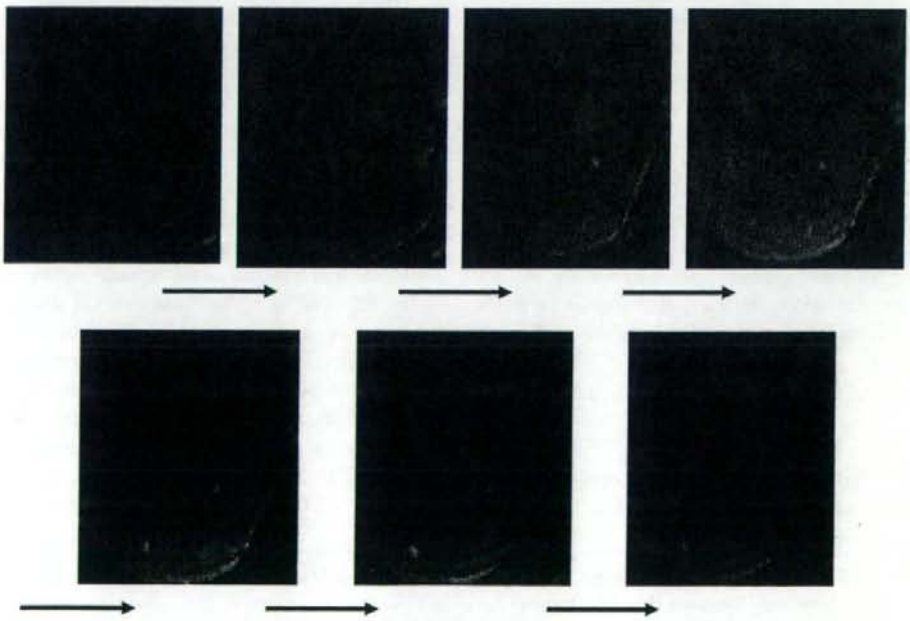

Figure 3. Dynamic MR study on the tumor.

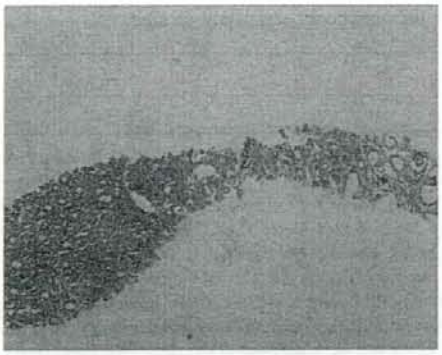

Figure 4. HCC tissue obtained by aspiration biopsy, showing the boundary between the two different structures of the tumor.

Figure 5. Gross appearance of the resected HCC nodule.

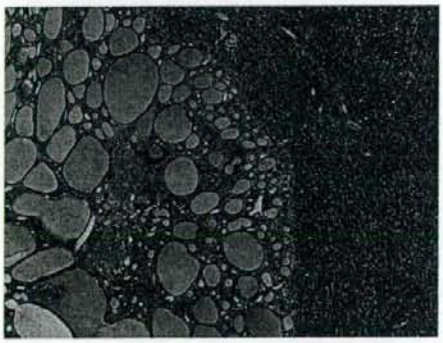

Figure 6. The boundary of the different histological grades of HCC (magnification: ×40).

Figure 7. Well-differentiated HCC tissue (magnification: ×100).

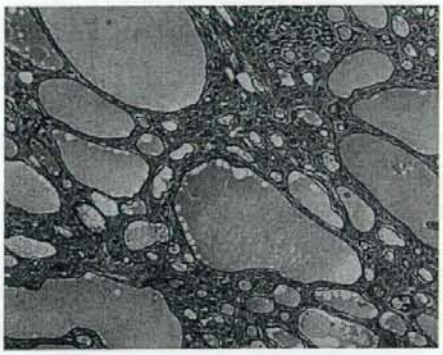

Figure 8. Moderately differentiated HCC tissue, showing the markedly dilated pseudoglands (magnification: ×100).

and hyperintense subnodule in the center of the tumor, and surrounded by a hypoechoic tumor area consisted of well-differentiated HCC without any fatty change. Possible causes for such atypical or inversed "nodule-in-nodule" appearance have not yet been fully discussed. A previous report demonstrated that the HCC hyperintensity on T2-weighted images is correlated with expansive growth, peliotic change, and hypervascularity (6), suggesting that the inner subnodule in the present case had different biological features. Indeed, the subnodule in our case showed a marked hyperintensity on T2-weighted images, but it was not clearly enhanced by contrast media. The unidentified substance within peliotic change-like dilated pseudoglands might contribute to the MR imaging findings seen in our case.

Although the precise mechanism of hyperechogenicity for the inner nodule in this case remained unclear, it is noteworthy that hyaline cast deposition within the collecting tubules in the kidney of the newborns accounts for the US finding of hyperechoic renal pyramids (7). Thus, it was possible that the hyperechogenicity of the inner nodule reflected the pinkish substance reminiscent of an amorphous hyaline in the dilated pseudoglands. The inner substance was also described as colloid-like material (8). Indeed, the large pseudoglandular structure resembles thyroid follicles, and the thyroid adenoma with colloid type follicles is often demonstrated as hyperechoic (9). From these points of view, it is speculated that the degree of hyperintensity and hyperechogenicity may, at least in part, be dependent on not only the size of the peliotic change-like dilated pseudoglands but also the nature of substances within the pseudoglands.

When we encounter HCC, featuring an atypical or inversed "nodule-in-nodule" appearance, we should pay care-

ful attention to its unique pathological architecture in addition to the commonly-seen fatty change.

References

1. Eguchi A, Furuta T, Haraguchi M, Sugimachi K. Early stage hepatocellular carcinoma detected during intraoperative ultrasonography. Am J Gastroenterol **89**: 595-598, 1994.
2. Yamagata M, Masaki T, Okudaira T, et al. Small hyperechoic nodules in chronic liver diseases include hepatocellular carcinomas with low cyclin D1 and Ki-67 expression. Hepatology **29**: 1722-1729, 1999.
3. Kutami R, Nakashima Y, Nakashima O, Shiota K, Kojiro M. Pathomorphologic study on the mechanism of fatty change in small hepatocellular carcinoma of humans. J Hepatol **33**: 282-289, 2000.
4. Kojiro M. Pathology of early hepatocellular carcinoma: progression from early to advanced. Hepatogastroenterology **45** Suppl 3 : 1203-1205, 1998.
5. Ogata R, Majima Y, Tateishi Y, et al. Bright loop appearance; a characteristic ultrasonography sign of early hepatocellular carcinoma. Oncol Rep **7**: 1293-1298, 2000.
6. Honda H, Kaneko K, Maeda T, Kuroiwa T, Fukuya T. Small hepatocellular carcinoma on magnetic resonance imaging. Relation of signal intensity to angiographic and clinicopathological findings. Invest Radiol **32**: 161-168, 1997.
7. Salisz JA, Kass EJ, Cacciarelli AA. Transient acute renal failure in the neonate. Urology **41**: 137-140, 1993.
8. Anthony PP. Tumours and tumor-like lesions of the liver and biliary tract: aetiology, epidemiology and pathology. In: Pathology of the Liver. 4th ed. MacSween RNM, Burt AD, Portmann BC, Ishak KG, Scheuer PJ, Anthony PP, Eds. Churchill Livingstone, London, 2002: 711-775.
9. Chang TC, Hong CT, Chang SL, Hsieh HC, Liaw KY, How SW. Correlation between sonography and pathology in thyroid diseases. J Formos Med Assoc **89**: 777-783, 1990.

Transarterial chemoembolization as salvage therapy after unsuccessful hepatic arterial infusion chemotherapy in advanced hepatocellular carcinoma

KAZUTA FUKUMORI[1], YOICHI YANO[2], EIJI ANDO[1], SHUJI SUMIE[1], KOTORO KUWAKI[1], FUMIHIKO YAMASHITA[2], MASATOSHI TANAKA[1] and MICHIO SATA[1]

[1]Division of Gastroenterology, Department of Internal Medicine, Kurume University School of Medicine, 67 Asahi-machi, Kurume-shi, Fukuoka-ken 830-0011; [2]Department of Internal Medicine, Saga Social Insurance Hospital, 3-8-1 Hyogo-Minami, Saga-shi, Saga-ken 849-8522, Japan

Received January 14, 2008; Accepted March 31, 2008

Abstract. The prognosis for advanced hepatocellular carcinoma (HCC) remains unsatisfactory. Transarterial chemoembolization (TACE) and/or hepatic arterial infusion chemotherapy (HAIC) have been reported to be useful options. However, there are few reports of salvage therapies for patients without a curative response to initial chemotherapy. The aim of this study was to elucidate the efficacy of additional TACE as salvage therapy in cases of advanced HCC which failed to respond to HAIC. Of 43 patients with advanced HCC who did not show a complete response (CR) to HAIC, 12 were treated with additional TACE as salvage therapy (Group A). The rest were enrolled as disease control subjects (Group B). Response rates and prognosis were compared. For HAIC, cisplatin (10 mg/body on days 1-5) was administered. Subsequent treatment was the infusion of 5-fluorouracil (250 mg/body on days 1-5), which was scheduled for 4 serial courses. For TACE, carboplatin (150 mg/body) or epirubicin (30 mg/body) was administered mixed with 3 ml of ethiodized oil every 4 weeks. A CR or PR, ST and PD were observed in 6, 3, and 3 patients in Group A and 13, 18 and 0 patients in Group B, respectively. The difference in response between the two groups was significant (P=0.0074). The 1-, 2- and 3-year survival rates were 83.3, 75.0 and 44.4% in Group A and 83.9, 41.5 and 11.3% in Group B, respectively. Patients in Group A had a better prognosis than did those in Group B (P=0.018). Median survival was 31.9 months (5.8-41.1) in Group A and 16.2 months (3.3-53.2) in Group B. Consequently, TACE as salvage therapy after HAIC may improve the prognosis for patients with advanced HCC.

Correspondence to: Dr Kazuta Fukumori, Division of Gastroenterology, Department of Internal Medicine, Kurume University School of Medicine, 67 Asahi-machi, Kurume-shi, Fukuoka-ken 830-0011, Japan
E-mail: kazuta.f@d8.dion.ne.jp

Key words: hepatocellular carcinoma, transarterial chemoembolization, hepatic arterial infusion chemotherapy, additional therapy

Introduction

Hepatocellular carcinoma (HCC) is one of the most common cancers in the world. While surveillance programs for chronic liver diseases have led to early diagnosis and effective treatments, the prognosis for advanced HCC remains unsatisfactory. Transarterial chemoembolization (TACE) has been shown to be a palliative treatment with evidence of survival benefit (1,2). Recently, improvements in an implantable drug delivery system have enabled repeated arterial infusion of chemotherapeutic agents for patients with advanced HCC. Although the optimal doses, schedule and types of chemotherapy used in conjunction with this system have not been fully established, an improvement in response rates and survival has been reported (3-8). We reported on the usefulness of hepatic arterial infusion chemotherapy (HAIC) using cisplatin (CDDP) and 5-fluorouracil (5-FU) for advanced HCC with portal vein tumor thrombosis (PVTT) (9,10). However, there are few reports on the best salvage treatment for patients who do not achieve a complete response to the initial chemotherapy. The aim of this study was to elucidate whether additional TACE as salvage therapy after unsuccessful HAIC affects the prognosis of patients with advanced HCC.

Patients and methods

Patients. Ninety-two patients with advanced HCC were treated with HAIC using CDDP and 5-FU via a subcutaneously-implanted injection port at Saga Social Insurance Hospital between June 1990 and December 1997. HCC was diagnosed clinically using imaging studies including ultrasonography, computed tomography (CT), magnetic resonance imaging and celiac angiography, and tumor biopsy. Due to the advanced tumor stage or the coexistence of cirrhosis, these patients were not suitable for surgical resection or ablation therapy, such as percutaneous ethanol injection, microwave coagulation therapy or radio-frequency tumor ablation. The 11 patients who achieved a complete response (CR) to HAIC, 21 patients

Table I. Patient characteristics.

	Group A	Group B	P-value
Number	12	31	
Gender (male/female)	10/2	25/6	0.805
Age (years)[a]	65.2±8.8	64.5±8.6	0.843
Virus marker (anti-HCV/HBs Ag)	12/0	27/4	0.200
Child's classification[b] (A/B/C)	8/4/0	19/12/0	0.705
Tumor size (mm)[a]	41.8±21.5	53.6±22.6	0.126
Tumor stage[c] (II/III+IV)	3/9	9/22	0.785
Serum α-fetoprotein (ng/ml)[a]	5,128±13,488	2,463±7,549	0.414
Serum des-g-carboxy prothrombin (mAU/ml)[a]	2,222±6,928	3,282±11,744	0.771
Pre-treatment (none/PEIT/TACE/MCT/resection)	7/2/2/1/0	10/6/10/4/1	0.168

[a]Data are the mean ± SD. [b]Based on the criteria of Child and Turcotte (11). [c]According to TMN classification (18). Anti-HCV, antibody for hepatitis C virus; HBs Ag, hepatitis B surface antigen; PEIT, percutaneous ethanol injection therapy; TACE, transarterial chemoembolization; MCT, microwave coagulation therapy; HAIC, hepatic arterial infusion chemotherapy.

who developed PVTT and 17 patients whose hepatic reserve was classified as Child's classification Grade C were excluded from the study (11). The remaining 43 patients were enrolled and divided into two groups: Group A, 12 patients treated with additional TACE as salvage, and Group B, 31 patients who did not receive TACE. Table I summarizes the clinical profiles of the patients in each group. There were no significant differences in the clinical profiles between the two groups.

Technique of catheter placement. A catheter was inserted through the femoral artery using the Seldinger method. Following the detection of HCC, an indwelling 4- or 5-French heparin-coated catheter was put in place, with the tip of the catheter being inserted in the common or proper hepatic artery. The right gastric artery and the gastroduodenal artery were occluded with steel coils to prevent any gastroduodenal injury following administration of the anticancer agents. The other end of the catheter was connected to an injection port, and the device was implanted into a subcutaneous pocket in the lower right quadrant. The entire procedure was performed under local anesthesia. In order to prevent the occlusion of the device, 5 ml (5000 units) of heparin solution was injected biweekly.

Chemotherapeutic regimen of HAIC. One course of HAIC consisted of the daily administration of CDDP (10 mg/h on days 1-5) followed by the infusion of 5-FU (250 mg/5 h on days 1-5) using a mechanical infusion pump via a subcutaneously-implanted injection port. In principle, the patients were to receive HAIC for four serial courses every 6 weeks. A serotonin antagonist, andansetron hydrochloride, was administered intravenously as an antiemetic, and saline infusion (500 ml) was administered during the chemotherapy infusion.

Transarterial chemoembolization as salvage therapy. TACE was administered as salvage therapy to those patients who consented to additional therapy and whose response to HAIC was classified as partial response (PR), stable disease (ST) or progressive disease (PD). A lipiodol emulsion, 3 ml of ethiodized oil (Lipiodol), carboplatin (150 mg/body) or epirubicin (30 mg/body), was injected slowly through the indwelling injection port under fluoroscopy. TACE was repeated every 4 weeks until one of the following signs was noted: i) disappearance of all viable HCC on enhanced CT, ii) an apparent increase in the tumor diameter or the appearance of portal vein tumor thrombosis, or iii) deterioration of hepatic function. The total doses of carboplatin and epirubicin were set at 1500 mg and 300 mg, respectively. In this study, a gelatin sponge was not used in order to avoid the deterioration of liver function (8,12).

Response criteria. Tumor response to HAIC was evaluated in both groups, and tumor response to TACE was evaluated in Group A. Local response to treatment was classified based on the criteria defined by the World Health Organization: CR, complete disappearance of all known disease and the appearance of no new lesions as determined by two observations not less than 4 weeks apart; PR, >50% reduction in the total tumor load of all measurable lesions determined by two observations not less than 4 weeks apart; ST, does not qualify as CR/PR or PD; and PD, a >25% increase in the size of one or more measurable lesions or the appearance of one or more new lesions.

Adverse events. Adverse events were graded according to the Common Terminology Criteria for Adverse Events v3.0 (13).

Statistical analysis. Data were expressed as the means ± SD. The χ^2 test, Fisher's exact probability test, the Student's t-test and Welch's t-test were used to compare patient characteristics and tumor response to HAIC. Cumulative survival rates were calculated using the Kaplan-Meier method. Statistical differences were considered significant at $P<0.05$.

This study was approved by the Ethics Committee of the Saga Social Insurance Hospital.

Table II. Response to treatment.

	Group A (n=12)		Group B (n=31)
	HAIC	HAIC and TACE	HAIC
CR	0	1	0
PR	3	5	13
ST	8	3	18
PD	1	3	0
P-value	0.483	0.0074	

Abbreviations as in Table I. Group A, patients receiving HAIC followed by TACE; Group B, patients receiving HAIC only. CR, complete response; PR, partial response; ST, stable disease; PD, progressive disease.

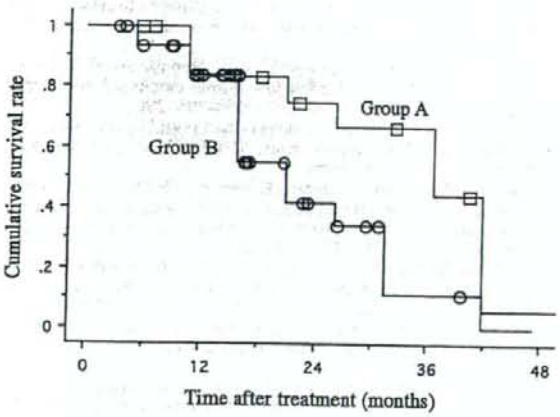

	Survival Rate (%)				Median survival (months)
	1-year	2-year	3-year		
Group A	83.3	75.0	44.4	P=0.018	31.9
Group B	83.9	45.1	11.3		16.2

Figure 1. The cumulative survival rate of patients with advanced hepatocellular carcinoma who received hepatic arterial infusion chemotherapy only (Group B, n=31) and those who received the same treatment followed by transcatheter arterial chemoembolization (Group A, n=12). The survival rate was significantly longer for patients in Group A than in Group B (P=0.018).

Results

The patients in Groups A and B received 5.75±2.60 and 5.89±3.30 courses of HAIC, respectively. TACE was performed for 5.66±1.9 courses in the Group A patients. As shown in Table II, CR+PR, ST and PD were observed in 6, 3 and 3 patients in Group A and 13, 18 and 0 patients in Group B, respectively. The difference in tumor response between the two groups was significant (P=0.0074). Three patients in Group A responded to TACE although they had failed to respond to HAIC, including one CR case.

As shown in Fig. 1, the 1-, 2- and 3-year survival rates were 83.3, 75.0 and 44.4% in Group A and 83.9, 41.5 and 11.3% in Group B, respectively. Patients in Group A had a better prognosis than did those in Group B (P=0.018). The median survival was 31.9 months (5.8-41.1) in Group A, and 16.2 months (3.3-53.2) in Group B.

No severe adverse reactions or complications, such as hepatic abscess, severe myelosuppression or severe hepatic damage, occurred (Table III), although some patients needed minimal symptomatic treatments.

Table III. Response to treatment.

	Group A (n=12)	Group B (n=31)
Complications		
Catheter obstruction	2 (16)	4 (13)
Hematoma around injection port	1 (8)	5 (16)
Dislocation of the tip of the catheter	1 (8)	2 (6)
Infection around injection port	1 (8)	7 (22)
Obstruction of hepatic artery	0	1 (3)
CTCAE		
Nausea	Grade 1, 2 (16)	Grade 1, 6 (19)
Anorexia	0	Grade 2, 1 (3)
Mucositis-stomach	Grade 1, 1 (8)	Grade 1, 2 (6)
Ulcer, GI-stomach	0	Grade 2, 4 (13)
Ulcer, GI-duodenum	Grade 2, 1 (8)	Grade 2, 2 (6)
Fever[a]	Grade 1, 1 (8)	0
Diarrhea	0	Grade 1, 1 (3)

Data are expressed as the numbers of patients and (percentages). CTCAE, Common Terminology Criteria for Adverse Events v3.0 (13). [a]Peculiar to TACE.

Discussion

We evaluated the efficacy of additional TACE as a salvage therapy for patients with advanced HCC who did not achieve a complete response to HAIC. Since we did not use a gelatin sponge to avoid deterioration of hepatic reserve, the TACE employed in this study may be different from conventional TACE.

As for the administration of Lipiodol emulsion mixed with anticancer agents, its antitumor mechanisms have been reported to be the microembolization of tumor vessels and a slow release of anticancer agents (14-16). As shown in Table II, the tumor response rate (CR+PR for all cases) in Group A was comparable to that of Group B; the former was

50% and the latter 42%. However, patients in Group A had a better prognosis than did those in Group B; the median survival was 31.9 months in Group A and 16.2 months in Group B (Fig. 1). The exact reason for this observation is not at present clear. Repetitive microembolization of a tumor-feeding artery, which is unrelated to the drug sensitivities of the tumor cells, may retard the progression of HCC, although complete necrosis of the tumor is rare. Preservation of the hepatic arteries and hepatic reserve, which may have resulted from performing the treatments without a gelatin sponge, may also have played an important role in permitting repeated anticancer treatments. Three patients in Group A, considered to have ST following the administration of HAIC, responded to this salvage therapy and achieved CR or PR. While effective treatment for advanced HCC has not been established, particularly in patients without curative responses to initial chemotherapy, TACE without a gelatin sponge may prove to be a useful second therapeutic alternative.

However, in two patients in this study additional TACE resulted in a worsening of tumor stage. Akamastu *et al* (17) reported that TACE could lead to the development of poorly-differentiated HCC or multiple recurrences. TACE seems to be a double-edged sword when used in cases of advanced HCC. Consequently, after the administration of TACE, follow-up studies are needed for the early detection of HCC progression.

No severe adverse events related to TACE were observed, although the sample size of this study was small. In terms of quality of life issues, it was significant that all the patients who received TACE could be treated on an outpatient basis.

In conclusion, repetitive cycles of TACE without a gelatin sponge may be a useful salvage therapy for patients with advanced HCC who do not have portal vein tumor thrombosis. However, the use of both HAIC and TACE in advanced HCC has not been confirmed for populations worldwide. A randomized prospective control trial is required to confirm these findings.

References

1. Llovet JM, Real MI, Montana X, *et al*: Arterial embolization or chemoembolization versus symptomatic treatment in patients with unresectable hepatocellular carcinoma: a randomized control trial. Lancet 359: 1734-1739, 2002.
2. Lo CM, Ngan H, Tso WK, *et al*: Randomized controlled trial of transarterial lipiodol chemoembolization for unresectable hepatocellular carcinoma. Hepatology 35: 1164-1171, 2002.
3. Patt YZ, Charnsangavej C, Yoffe B, *et al*: Hepatic arterial infusion of floxuridine, leucovorin, doxorubicin, and cisplatin for hepatocellular carcinoma: effect of hepatitis B and C viral infection on drug toxicity and patient survival. J Clin Oncol 12: 1204-1211, 1994.
4. Toyoda H, Nakano S, Kumada T, *et al*: The efficacy of continuous local arterial infusion of 5-fluorouracil and cisplatin through an implanted reservoir for advanced hepatocellular carcinoma. Oncology 52: 295-299, 1995.
5. Minoyama A, Yoshikawa M, Ebara M, Saisho H, Sugiura N and Ohto M: Study of repeated arterial infusion chemotherapy with a subcutaneously implanted reservoir for advanced hepatocellular carcinoma. J Gastroenterol 30: 356-366, 1995.
6. Asahara T, Itamoto T, Katayama K, *et al*: Adjuvant hepatic arterial infusion chemotherapy after radical hepatectomy for hepatocellular carcinoma - results of long-term follow-up. Hepatogastroenterology 46: 1042-1048, 1999.
7. Okuda K, Tanaka M, Shibata J, *et al*: Hepatic arterial infusion chemotherapy with continuous low dose administration of cisplatin and 5-fluorouracil for multiple recurrence of hepatocellular carcinoma after surgical treatment. Oncol Rep 6: 587-591, 1999.
8. Sumie S, Yamashita F, Ando E, Tanaka M, Yano Y, Fukumori K and Sata M: Interventional radiology for advanced hepatocellular carcinoma: Comparison of hepatic arterial infusion chemotherapy and transcatheter arterial lipiodol chemoembolization. AJR Am J Roentgenol 181: 1327-1334, 2003.
9. Ando E, Yamashita F, Tanaka M and Tanikawa K: A novel chemotherapy for advanced hepatocellular carcinoma with tumor thrombosis of the main trunk of portal vein. Cancer 79: 1890-1896, 1997.
10. Ando E, Tanaka M, Yamashita F, *et al*: Hepatic arterial infusion chemotherapy for advanced hepatocellular carcinoma with portal vein tumor thrombosis. Cancer 95: 588-595, 2002.
11. Child CG and Turcotte JG: Surgery and portal hypertension. In: The Liver and Portal Hypertension. Child CG (ed). WB Saunders, Philadelphia, pp49-51, 1964.
12. Ueno K, Miyazono N, Inoue H, Nishida H, Kanetsuki I and Nakajo M: Transcatheter arterial chemoembolization therapy using iodized oil for patients with unresectable hepatocellular carcinoma. Cancer 88: 1574-1581, 2000.
13. Trotti A, Colevas AD, Setser A, *et al*: CTCAE v3.0: development of a comprehensive grading system for the adverse effects of cancer treatment. Semin Radiat Oncol 13: 176-181, 2003.
14. Konno T: Targeting chemotherapy for hepatoma: arterial administration of anticancer drugs dissolved in Lipiodol. Eur J Cancer 28: 403-409, 1992.
15. Yoshikawa M, Saisho H, Ebara M, *et al*: A randomized trial of intrahepatic arterial infusion of 4'-epidoxorubicin with Lipiodol versus 4'-epidoxorubicin alone in the treatment of hepatocellular carcinoma. Cancer Chemother Phamacol 33: S149-S152, 1994.
16. Ichida T, Kato M, Hayakawa A, *et al*: Theraputic effect of a CDDP-epirubicin-Lipiodol emulsion on advanced hepatocellular carcinoma. Cancer Chemother Phamacol 33: S74-S78, 1994.
17. Akamatsu M, Ishikawa T, Shiratori Y, *et al*: Factors predisposing to poorly differentiated hepatocellular carcinoma and its recurrence. Hepatogastroenterology 52: 391-397, 2005.
18. Hermanek P and Sobin LH: TMN Classification of Malignant Tumors. 4th edition, Springer Verlag, Berlin, pp59-61, 1987.

Annals of Surgical Oncology 15(5):1375–1382
DOI: 10.1245/s10434-008-9846-9

Microvascular Invasion in Patients with Hepatocellular Carcinoma and Its Predictable Clinicopathological Factors

Shuji Sumie, MD,[1] Ryoko Kuromatsu, MD,[1] Koji Okuda, MD,[2] Eiji Ando, MD,[1] Akio Takata, MD,[1] Nobuyoshi Fukushima, MD,[1] Yasutomo Watanabe, MD,[1] Masamichi Kojiro, MD,[3] and Michio Sata, MD[1]

[1]Division of Gastroenterology, Department of Medicine, Kurume University School of Medicine, 67 Asahi-Machi, Kurume, Fukuoka 830-0011, Japan
[2]Division of Hepato-Biliary-Pancreatic Surgery, Kurume University School of Medicine, 67 Asahi-Machi, Kurume, Fukuoka 830-0011, Japan
[3]Department of Pathology, Kurume University School of Medicine, 67 Asahi-Machi, Kurume, Fukuoka 830-0011, Japan

Background: Macroscopic vascular invasion is known to be a poor prognostic factor in hepatocellular carcinoma (HCC). The aim of this study was to determine the outcomes and predictive factors after hepatic resection for HCC with microvascular invasion (MVI).

Methods: One hundred ten patients who underwent curative resection for HCC without macroscopic vascular invasion were included in this retrospective study. The risk factors of these patients for recurrence-free and disease-specific survival were investigated, and the clinicopathological factors predicting the presence of MVI were also determined.

Results: Of the 110 resected specimens, 49 (45%) had evidence of MVI. By univariate analysis, MVI was found to be statistically significantly associated with greater tumor size, gross classification, histological grade, and intrahepatic micrometastasis. Gross classification proved to be the only independent predictive factor for MVI by multiple logistic regression analysis. By multivariate analysis, cirrhosis and MVI were identified as independent risk factors for recurrence-free survival. The 5-year recurrence-free survival rates for patients with and without MVI were 20.8% and 52.6%, respectively. By multivariate analysis, the number of tumors, presence of MVI, and intrahepatic micrometastasis were identified as independent predictors of disease-specific survival. The 5-year disease-specific survival rates for patients with and without MVI were 59.3% and 92.0%, respectively.

Conclusions: The presence of MVI was the most important risk factor affecting recurrence and survival in HCC patients after curative resection. Furthermore, this study showed that gross classification of HCC can be very helpful in predicting the presence of MVI.

Key Words: Hepatocellular carcinoma—Microvascular invasion—Gross classification—Hepatic resection—Recurrence—Survival.

Hepatocellular carcinoma (HCC) is one of the most common malignancies in the world. Recent advances in imaging procedures have led to increased detection of early-stage HCC and improved survival because of the greater number of patients identified in which curative hepatic resection is possible.[1,2] However, the long-term survival rate is still unsatisfactory as a result of the high rate of intra- and extrahepatic recurrences.[3,4] Tumor invasion in the portal and/or hepatic vein is associated with increased risk leading to early recurrences of HCC.[5–9] Moreover, the fatal recurrence of HCC with vascular invasion limits additional attempts at

Published online March 7, 2008.
Address correspondence and reprint requests to: Shuji Sumie, MD; E-mail: sumie_shyuuji@kurume-u.ac.jp

various curative therapies, such as hepatic resection, percutaneous ethanol injection, microwave coagulation therapy, and radiofrequency ablation, thereby contributing to poor survival.[10] Macroscopic vascular invasion, such as a tumor thrombus in the major portal vein, is known to be the crucial survival risk factor after resection or liver transplantation for HCC.[11–14] A previous study of natural history of HCC with macroscopic vascular invasion has shown a patient median survival time of 2.7 months.[15]

Microvascular invasion (MVI) is difficult to detect before treatment of HCC is undertaken, even if recent superior imaging procedures are used during patient evaluation. Although several studies have suggested that the presence of MVI is an independent factor predictive of poor survival after resection of HCC,[16–18] the significance of MVI is still unclear. The aim of this study was to evaluate whether the MVI of HCC is associated with tumor recurrence and affects patient long-term survival after curative resection, and to identify preoperative predictors of MVI.

PATIENTS AND METHODS

Patients

Between January 1995 and December 2005, 142 patients were diagnosed and underwent hepatic resection for HCC at the Kurume University School of Medicine. Patient inclusion criteria for this study were as follows: (1) patients with a single tumor up to 5 cm or three or fewer tumors each up to 3 cm, (2) patients without radiological evidence of macroscopic portal and hepatic vein tumor invasion, (3) patients without extrahepatic metastasis, and (4) patients who underwent curative hepatic resection defined as the removal of all macroscopic residual tumors. Of these 142 patients, 110 patients met these criteria and were retrospectively included in this study. There were 90 male (82%) and 20 female patients, with a mean age of 62.6 ± 10.5 years. With respect to viral markers, 74 patients (67%) were positive for hepatitis C virus (HCV) antibody, 27 patients (25%) were positive for hepatitis B surface antigen, and 9 patients were negative for both markers. Liver cirrhosis was present in 53 patients (48%). The mean maximum tumor size was 28.1 ± 9.6 mm, and 85 patients (77%) had a solitary tumor. In the surgical procedures, lobectomy, segmentectomy, and subsegmentectomy are anatomic resections of Couinaud's segment classification and were performed in 13, 50, and 22 patients, respectively. Partial hepatectomy is a nonanatomic resection consisting of less than subsegmentectomy and was performed in 25 patients.

Preoperative Evaluation

In 21 of 110 patients, preoperative diagnosis of HCC was histologically confirmed by needle biopsy under ultrasonographic guidance. In the remaining 89 patients, HCC was diagnosed on the basis of the findings of typical radiological features on ultrasonography, contrast-enhanced dynamic computed tomography (CT), and magnetic resonance imaging (MRI), along with high alfa-fetoprotein (AFP) and des-gamma-carboxy prothrombin (DCP) levels. The preoperative hepatic functional reserve was evaluated by the Child-Pugh scoring system[19] and the 15-minute retention rate for indocyanine green. Tumor size was determined on the basis of the largest dimension observed on ultrasonography and CT.

Histological Criteria

MVI was defined as microscopic tumor invasion identified in portal or hepatic vein of the surrounding liver tissue, which was contiguous to the tumor. Intrahepatic micrometastasis (IM) was defined as satellite micronodule in the surrounding liver tissue, which was isolated from the main tumor. Tumor differentiation was histologically graded according to the classification of the Liver Cancer Study Group of Japan.[20] Gross classification of nodular type HCC was based primarily on the definition of Kanai et al.[21] and the Liver Cancer Study Group of Japan[20]: vaguely nodular type (VN type, nodule has distinct margins and contains portal tracts), single nodular type (SN type, round nodule with clear demarcation), single nodular with extranodular growth type (SNEG type, similar to SN type but showing extranodular growth), and confluent multinodular type (CMN type, a nodule formed by a cluster of small and confluent nodules). The tumors of the 110 patients were classified grossly as VN type (3 tumors, 2.7%), SN type (59 tumors, 53.6%), SNEG type (29 tumors, 26.4%), and CMN type (19 tumors, 17.3%).

Patient Follow-up

After surgical resection, each patient was followed carefully. Serum biochemistries, AFP levels,